

Dispersion strengthening in vanadium microalloyed steels processed by simulated thin slab casting and direct charging

Part 1 – Processing parameters, mechanical properties and microstructure

Y. Li^{1,2}, J. A. Wilson³, A. J. Craven³, P. S. Mitchell², D. N. Crowther⁴ and T. N. Baker*¹

A study simulating thin slab continuous casting followed by direct charging into an equalisation furnace has been undertaken based on six low carbon (0.06 wt-%) vanadium microalloyed steels. Mechanical and impact test data showed that properties were similar or better than those obtained from similar microalloyed conventional thick cast as rolled slabs. The dispersion plus dislocation strengthening was estimated to be in the range 80–250 MPa. A detailed TEM/EELS analysis of the dispersion sized sub 15 nm particles showed that in all the steels, they were essentially nitrides with little crystalline carbon detected. In the steels V–Nb, V–Ti and V–Nb–Ti, mixed transition metal nitrides were present. Modelling of equilibrium precipitates in these steels, based on a modified version of ChemSage, predicted that only vanadium rich nitrides would precipitate in austenite but that the C/N ratio would increase through the two phase field and in ferrite. The experimental analytical data clearly point to the thin slab direct charging process, which has substantially higher cooling rates than conventional casting, nucleating non-equilibrium particles in ferrite which are close to stoichiometric nitrides. These did not coarsen during the final stages of processing, but retained their highly stable average size of ~7 nm resulting in substantial dispersion strengthening. The results are considered in conjunction with pertinent published literature.

Keywords: High strength low alloy steel, Direct charged thin slab process, Precipitation, Dispersion strengthening

Introduction

The dispersion strengthening contribution σ_p to the yield strength σ_y in high strength low alloy (HSLA) steels by carbide, nitride and/or carbonitride particles has been discussed for over 40 years. Most of the interest has been in steels containing niobium and/or vanadium additions. Values of σ_p have been calculated based on the Ashby–Orowan equation,^{1,2} which assumes that the particles are incoherent and randomly dispersed. The particles size $d(=2r)$ and volume fraction f are the main variables which are influenced by the chemical composition of the

steel and the processing parameters. Normally, particle stoichiometry has also been assumed. Gladman *et al.*^{3,4} found a satisfactory agreement between the values of σ_p estimated using the Ashby–Orowan approach,^{1,2} substituting their experimental data for r and f ,³ and the indirect approach based on the Hall–Petch relationship.^{5,6} Usually, dislocation strengthening σ_d was either ignored or considered to be low and was assumed to be included in σ_p . For example, in 0.1 wt-%C steels, with typical levels of 0.15 wt-%V or 0.04 wt-%Nb, with an average r of 5 nm, σ_p was estimated to be about 100–150 MPa. These figures are within the range expected for HSLA steels, continuously cast to 200–250 mm thick slabs and controlled rolled to ~5 mm strip.⁷

More recently, attention has focused on thin slab (30–80 mm) direct charged (TSDC) steels, where higher cooling rates occur, for example, 18 K s⁻¹ between the finish rolling temperature (FRT), which is normally ~850°C, and the end of water spray cooling, 550–650°C. Thus conditions far from equilibrium exist. Previous

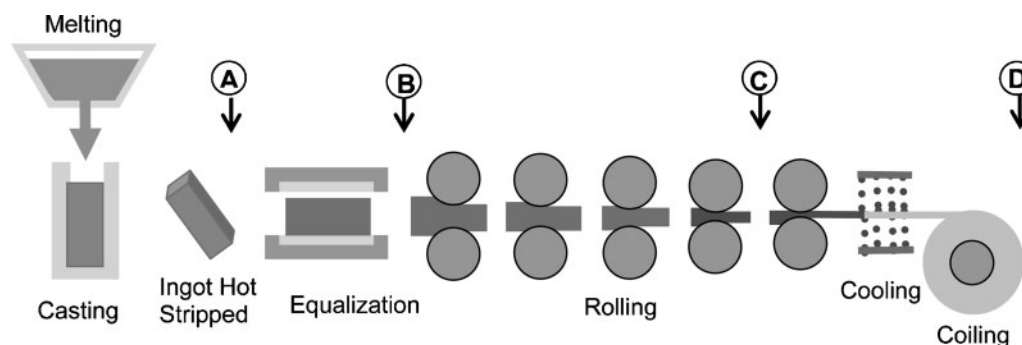
¹Metallurgy and Materials Engineering Group, Department of Mechanical Engineering, University of Strathclyde, Glasgow G1 1XJ, Scotland, UK

²VANITEC, Winterton House, High Street, Westerham, Kent TN16 1AQ, UK

³Department of Physics and Astronomy, University of Glasgow, Glasgow, G12 8QQ, Scotland, UK

⁴Corus Group, Swinden Technology Centre, Rotherham, S60 3AR, UK

*Corresponding author, email neville.baker@strath.ac.uk



1 Schematic diagram showing process route used for simulating thin slab direct charging

publications by the present authors^{8,9} have reported that in TSDC steels, depending on the equalisation and end cool temperatures, combined contributions of dispersion and dislocation strengthening to the yield strength can reach 250 MPa. It is therefore of interest to ascertain if the TSDC process route modifies the dispersion strengthening particle chemical composition, size range or volume fraction, which could lead to higher values of σ_p . Because of the small ferrite grain size developed, an acceptable level of toughness is maintained.

Thin slab continuous casting followed by direct charging into an equalisation furnace has the potential to replace the traditional thick slab casting process for the production of thin sheet HSLA steel. Capital costs and plant size are reduced because fewer rolling stands are required and no space is needed to store cast slabs before rolling.¹⁰ The smaller number of rolling stands and the removal of the need to reheat thick slabs from ambient temperature also leads to reduced energy consumption.¹¹ The ability to change the composition of the melts quickly enables a rapid response to be made to changes in the market demand for different grades of steel, making the plant more competitive. Also, the use of electric arc furnaces enhances the ability to recycle scrap steel and reduces emissions from the plant.¹² Thus, both economically and environmentally, the thin slab direct charged (TSDC) process offers very significant benefits over the conventional process.¹³ However, the thermomechanical conditions in the direct process are radically different to those in the conventional process. The slab is much thinner and so the cooling rates are much faster, which potentially leads to segregation effects from dendritic solidification.^{14,15} Because the thin slab is directly charged, it no longer undergoes the $\gamma \rightarrow \alpha \rightarrow \gamma$ phase transitions that occur when a conventional thick slab is cooled to ambient temperature and then reheated before rolling. This will modify the elemental distributions and may modify any precipitation that occurs before rolling.¹⁶ Finally, much less mechanical deformation is required so that there is a possibility that the as cast structure has a greater effect on the final microstructure than in the conventional process.

Previous papers by the present authors on TSDC microalloyed vanadium steels have considered the effect of chemical composition of the steel and processing conditions on the mechanical properties.^{8,9,15} In addition, the microstructural evolution from the as cast steel to the final product has been investigated.^{17–20} This paper, Part 1, is concerned with the effect dispersion strengthening vanadium precipitates have on the

mechanical properties and microstructure of TSDC microalloyed vanadium steels.

The thermodynamics and kinetics of precipitate formation are also considered in greater detail. In Part 2, details of the electron energy loss spectroscopy (EELS) quantitative chemical analysis of these particles including the light elements, down to a size of 4 nm, is presented.

Experimental techniques

The work was undertaken on six related low carbon (~ 0.06 wt-%), vanadium steels processed using a simulated TSDC process carried out at the Corus Swinden Technology Centre and shown schematically in Fig. 1.

All six steels contained ~ 0.1 wt-%V. Steel V was the baseline steel with ~ 0.007 wt-%N. Steel V–N had an increased N level of ~ 0.02 wt-%. Steel V–Ti had ~ 0.010 wt-%Ti and ~ 0.017 wt-%N. The three final steels had ~ 0.01 wt-%N with steel V–Nb having ~ 0.03 wt-%Nb, steel V–Nb–Ti having ~ 0.03 wt-%Nb and ~ 0.007 wt-%Ti, and steel V–Zr having ~ 0.008 wt-%Zr. In addition, the steels typically contained the following levels (in wt-%) of other elements Si (0.4), Mn (1.5), P (0.015), S (0.005), Cr (0.08), Mo (0.02), Ni (0.07), Al (0.025), B (< 0.0005), Cu (0.07), O (0.007).

The steels were melted in air as ~ 18 kg loads and cast into three moulds to produce 50 mm thick ingots. The typical cooling rate at the mid thickness position of the ingots was 3.5 K s^{-1} . The ingots were hot stripped from the mould and transferred directly to an equalising furnace set at one of three equalisation temperatures (1050, 1100 or 1200°C) and held for 30–60 min before rolling. After equalisation, the ingots were rolled on a laboratory reversing mill to 7 mm strips in five passes, which gave a total reduction of 86%. A typical rolling schedule is given in Table 1. The usual interpass time was 6 s. After the fourth pass, the strip was held for 25–40 s until a temperature of $\sim 870^\circ\text{C}$ was reached. Finish rolling temperatures varied from 880 to 850°C and the total rolling times were in the range of 75–90 s. After rolling, the strip was cooled under water sprays to simulate run-out table cooling, the cooling rate being $\sim 18 \text{ K s}^{-1}$. The target for the end cool temperature of the strip was in the range 550 – 650°C but occasionally process difficulties were encountered which took it out of this range. Following cooling, the strips were immediately put into a furnace set at 600°C and slow cooled to simulate coiling with an average cooling rate of 35 K h^{-1} from 600 to 400°C . The rolling schedule¹⁵ (Table 1) shows that most of the deformation was introduced at temperatures $> 1000^\circ\text{C}$ and that only the

Table 1 Rolling schedule typical of that used in this work

Pass no.	Mill setting, mm	Deformation per pass, %	Equalisation temperature, °C		
			1200	1100	1050
			Entry rolling temperature, °C		
1	40	20	1098	1019	978
2	30	25	1088	1013	978
3	20	33	1075	1007	973
4	12	40	1059	1002	972
5	7	42	859	850	862
Typical finish rolling temperature, °C			850	850	850

final pass was likely to fall within the temperature range which involved strain induced precipitation in austenite, which is known to be important in Nb steels, but less so in V steels. Samples of the steel were taken and water quenched after casting (A), after equalisation (B) and after the fourth rolling pass (C). The fourth sample was taken from the final product (D).

Specimens for mechanical and toughness testing were taken from the final product.^{8,9,15} Samples were prepared for optical metallography by standard metallographic techniques, and then etched in 2% nital. The ferrite grain size in the final strip was measured using a linear intercept method with an optical microscope attached to an image analyser, and 250 intercepts were counted.

Carbon extraction replicas were produced from the quarter thickness positions of the final 7 mm strip of the fully processed steels. Metallographically prepared specimens were etched with 2% nital before evaporating a thin carbon film onto its surface. Following stripping in 5% nital, the films were washed in methanol and distilled water before being deposited onto Cu mesh grids. The replicas were examined by analytical

transmission electron microscopy using a Philips EM400T with an EDAX Phoenix energy dispersive X-ray (EDX) system. The experimental details are given elsewhere.^{17,18} Two hundred small particles (≤ 25 nm) extracted onto the carbon replicas were counted for the size distribution of steel V–N, following processing at 1050/750°C, as shown in Table 2. Thin foils were also studied.

Results

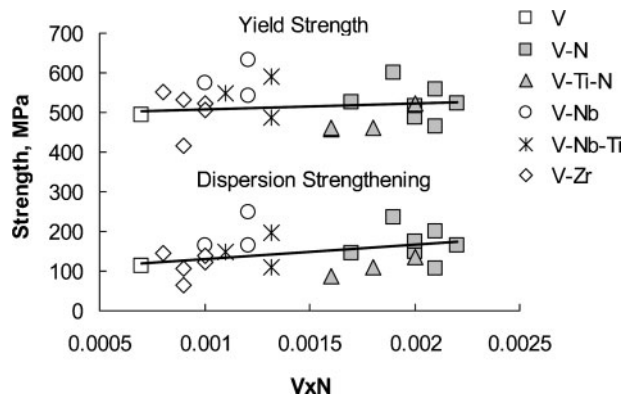
Mechanical and toughness properties

The mechanical and toughness properties are given in Table 2. The influence of the steel compositions and processing parameters on the yield stress and Charpy data have been considered in detail previously.^{8,9} Here the data for $\sigma_p + \sigma_d$ are of particular relevance. Using a modified version of the Hall–Petch equation, an estimate of the combined effect of the strengthening conferred by dispersed incoherent particles and by dislocation strengthening σ_d can be obtained. Equation (1) shows that by subtracting the ferrite lattice friction stress and C+N in solution (σ_o), together with the solid solution

Table 2 Mechanical properties of steels

Steel	Condition			Tensile properties					Charpy toughness	
	Equalisation temperature, °C	End cool temperature, °C	α grain size, μm	LYS, MPa	UYS, MPa	UTS, MPa	EL, %	$\sigma_p + \sigma_d$, MPa	J (at –20°C)	13J (ITT °C)
V	1100	603	5.6	493	528	617	24	113	72	–100
	1200	537	Bainite	560	540	671	17	–	23	–45
V–N	1050	602	6.2	557		664	24	200	43	–85
		750	6.2	521	544	641	15	163	36	–80
		764	6	466	484	555	10	106	68	–75
	1100	511	5.7	600	606	703	20	236	20	–45
		720	5.3	527	570	644	24	145	35	–45
	1200	646	7.2	489	492	631	19	149	27	–40
V–Ti	1050	700	6.8	518	529	642	20	173	37	–60
		590	5.7	463	500	579	22	86	68	–120
		609	6	459	482	578	26	87	71	–120
	1100	537	4.8	522	526	609	18	137	43	–90
V–Nb	1200	643	6.6	461	462	571	27	110	45	–100
	1050	693	4.5	574	632	674	23	166	52	–105
	1100	647	5.8	544	580	653	17	166	45	–100
V–Nb–Ti	1200	558	5.5	632	655	740	19	247	39	–95
	1050	678	5.9	487	553	599	24	109	76	–75
	1100	603	4.8	547	609	646	24	147	63	–100
V–Zr	1200	504	5.2	590	625	695	20	197	43	–90
	1050	556	4.2	531	554	631	25	107	54	–80
	1100	592	4.8	524	556	623	24	123	46	–80
	1200	678	6.2	508	516	619	26	140	36	–62
		750	7.8	416	430	543	25	64	59	–70
		642	4.8	552	576	655	22	145	30	–80

UYS – upper yield strength, LYS – lower yield strength; UTS – ultimate tensile strength; EL – elongation, ITT – infiltration transient temperature.



2 Effect of solubility product [V] [N] on strength

σ_s and grain size strengthening σ_g components from the measured lower yield strength σ_y , values of $\sigma_p + \sigma_d$ can be calculated. Equations (2) to (4)²¹⁻²⁴ gave σ_o , σ_s and σ_g

$$\sigma_p + \sigma_d = \sigma_y - (\sigma_o + \sigma_s + \sigma_g) \tag{1}$$

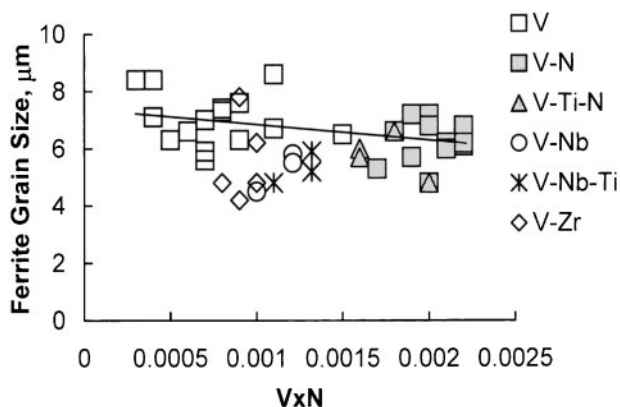
$$\sigma_o = 45 \text{MPa} \tag{2}$$

$$\sigma_s = 84(\text{Si}) + 32(\text{Mn}) + 38(\text{Cu}) + 43(\text{Ni}) \tag{3}$$

$$\sigma_g = 18 \cdot 1 D^{-1/2} \tag{4}$$

where D is the average ferrite grain size.

The values of $(\sigma_p + \sigma_d)$ estimated using the method described above for the present steels are given in Table 2 and shown in Fig. 2 as a function of the solubility product, VxN. In this analysis, it was assumed that strengthening from dislocations and texture was low and similar for all the steels examined. Dislocation densities observed in foils in the present work, supported this view. The data in Fig. 2 and Table 2, show that for specimens with comparable equalisation and end cool temperatures, the addition of titanium to vanadium or vanadium–niobium steels results in a decrease in the lower yield strength and dispersion strengthening, but a corresponding improvement in the Charpy toughness. This was because V–Ti nitrides formed at higher temperatures in austenite owing to the lower solubility of these compounds than V nitrides.⁴

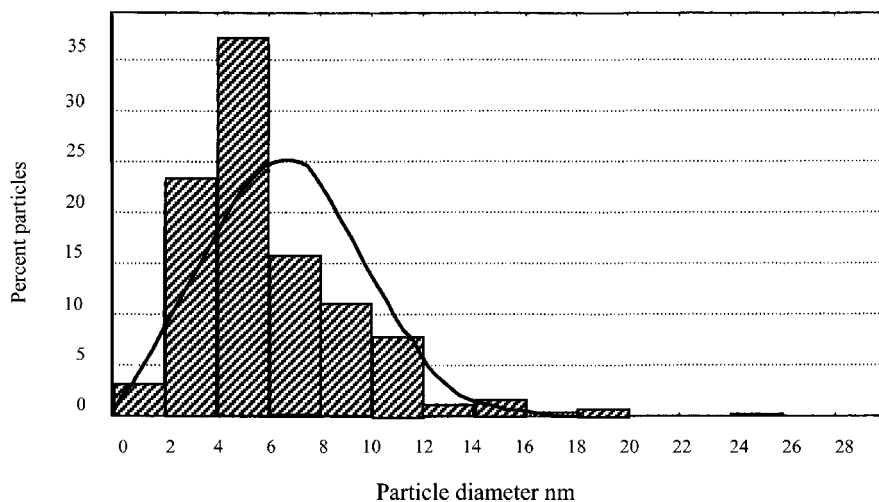


3 Relationship between VxN and ferrite grain size

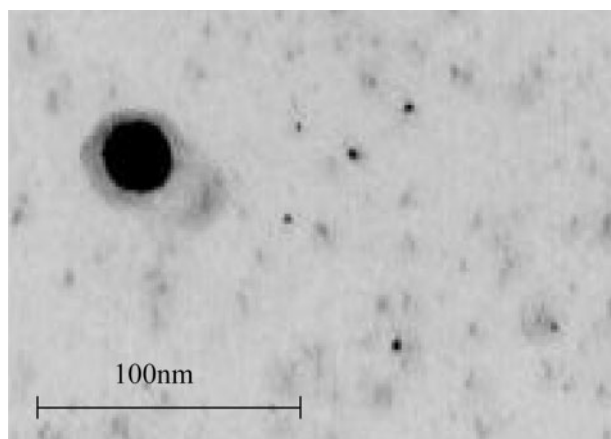
Microstructure

Ferrite grain sizes of a few micrometres were obtained in the final product. Figure 3 shows a graph of ferrite grain size plotted against the product of VxN. There is a general trend for the grain size to decrease as the solubility product VxN increases in steels V and V–N. Some values of the multiple microalloyed steels follow the same trend, while the addition of Nb or Ti, under some processing conditions, lead to a smaller grain size than the median.⁹ These results suggest that the recrystallisation stop temperature in the present TSDC process is low. Cuboidal particles 10–80 nm, which nucleated on the austenite grain boundaries, plus cruciforms, up to 150 nm in size in Ti containing steels, played an important role in the grain refinement.¹⁹

Fine precipitates, in the size range 4–15 nm, were only observed in the final product of each of the steels. An example of an experimentally determined size distribution for small particles is shown in Fig. 4. The largest number appears in the 4–6 nm range, but because the histogram is skewed to the right, the average particle size is 6.5 nm. The particles appear to be nucleated homogeneously, as shown in Fig. 5, but distributed throughout the matrix, inhomogeneously. Figure 6 is a dark field micrograph taken from a carbon extraction replica, which shows an area on the left hand side, which appears to be free of particles, whereas the right hand area in the same grain contains a random dispersion.



4 Experimentally determined size distribution for small particles for steel V–N, equalisation temperature 1050°C and end cool temperature 750°, with average particle diameter of 6.5 nm

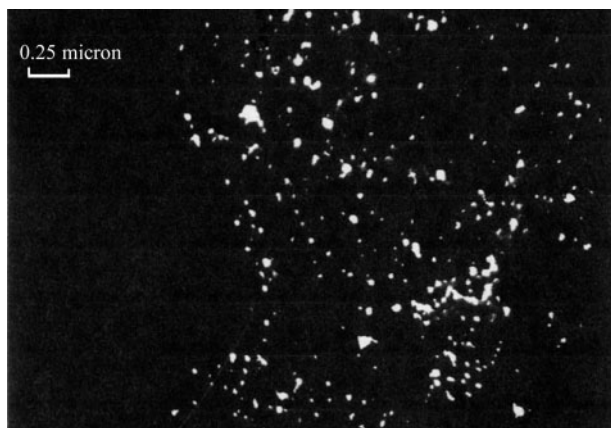


5 Small precipitates in size range 4–15 nm with one larger cuboid particle

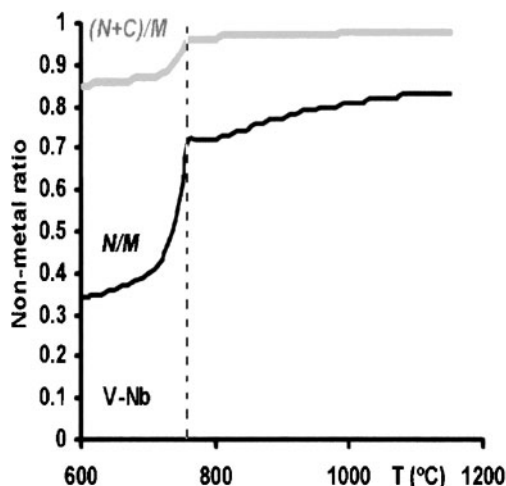
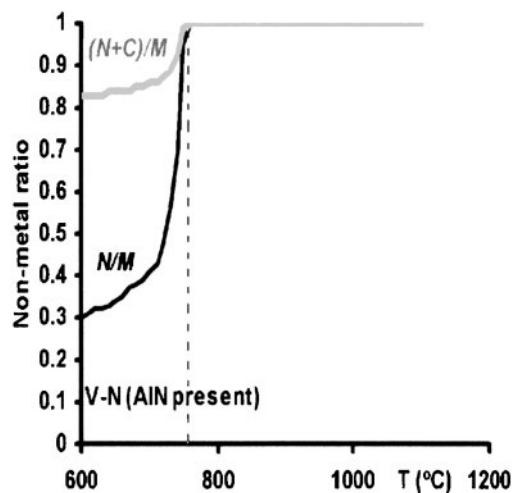
The details of the method of determining the composition of the particles and the problems which might arise through changes in the particle composition during the analysis, will be considered in Part 2.

Modelling

The particle composition versus temperature was modelled under equilibrium conditions for the target compositions of all steels using the ChemSage thermodynamic software package with a database modified by A. J. Rose of the Corus Swinden Technology Centre, Rotherham.²⁵ Fe_3C was included in the calculation but AlN formation was suppressed, because it was not observed experimentally. The exception to this was steel V–N where AlN was observed following an equalisation temperature of 1050°C but not at higher equalisation temperatures.⁹ Examples of the calculated solution temperatures for steels V–N and V–Nb are shown in Fig. 7, which also indicate that the particles forming at temperatures above the $\gamma \rightarrow \alpha$ transition temperature in steel V–N are predicted to be stoichiometric nitrides. Figure 7b shows that the particles forming above the $\gamma \rightarrow \alpha$ transition temperature of steel V–Nb contain some carbon, with the C/M ratio increasing from 0.15 to 0.25 as the temperature falls from the solution temperature to the $\gamma \rightarrow \alpha$ transition temperature. The calculations for steel V–Nb–Ti give similar results.



6 Dark field micrograph which shows grain on left hand side, which appears to be free of particles, whereas right hand grain contains random dispersion



7 ChemSage modelling of vanadium precipitates in austenite for steels V–N and V–Nb

Below the $\gamma \rightarrow \alpha$ transition temperature, a sharp rise in the C content, i.e. the difference between $(N+C)/M$ and N/M in Fig. 7, is predicted. With the exception of steel V–Ti, the particles are all predicted to have C/M of ~ 0.5 and $(C+N)/M$ of ~ 0.85 at 600°C , the target end cool temperature, i.e. carbon rich, slightly substoichiometric carbonitrides.

The modelling described above is for equilibrium conditions. However, the particle analysis presented in 'Part 2', clearly shows that they are essentially vanadium nitrides, suggesting a pronounced departure from equilibrium conditions. There have been some attempts to model non-equilibrium conditions. Most are concerned with niobium microalloyed steels and involve strain induced precipitation in austenite and the effect on recrystallisation, for example references.^{26,27} Strain induced precipitation was also found to be important in the nucleation kinetics of Ti carbonitride in austenite.²⁸ Akben *et al.*²⁹ compared the relative effectiveness of vanadium and niobium in solution on retarding dynamic precipitation in austenite. They interpret their results as indicating the greater effectiveness of Nb compared with V, when both are in solution, in retarding recrystallisation. This leads to recrystallisation preceding precipitation of VN in V steels whereas recrystallisation is more strongly retarded by the Nb in solution.²⁹ Thus the former would appear to be the situation in the present work. Another approach to

microstructural evolution has been described by Bratland *et al.*³⁰ who modelled diffusion controlled precipitation using a combination of chemical thermodynamics and kinetic theory. However, the thermodynamic model is based on solubility product data dependent on equilibrium conditions.

In an attempt to model a non-equilibrium situation, the present authors have used ChemSage software to estimate the particle volume fraction, knowing the particle composition determined from the EELS data, described in Part 2. This gave the particle analysis for vanadium nitrides close to stoichiometric VN with little C. Modelling of steel compositions was based on steel V–N, with levels of carbon 0.06, 0.01 and 0.001 wt-%, with the same level of all the other elements given above to examine the level of agreement compared with the EELS particle analysis data. The results are collated in Table 3, which shows the predicted volume fractions of VN and VC. Lowering the carbon from 0.06 to 0.01 wt-%C has a small effect on the volume fractions, but a significant change is predicted when the carbon is reduced to 0.001 wt-%. The volume fraction, *f*, of VN, after 1050°C equalisation, increased to become 88% of the total, compared with ~20% at 0.06 wt-%C. The results given in Table 3 show that the main outcome of lowering the carbon content in the steel from 0.06 to 0.001%, to approach that given by the EELS analysis of the vanadium particles, is the large decrease in the total volume fraction of particles precipitated in ferrite and as expected, an increase in the ratio of the volume fraction of VN particles to the total volume fraction of vanadium containing particles precipitated in ferrite, with the same changes in carbon content. Irrespective of the carbon content, assuming that all the nitrogen is combined with vanadium, the maximum volume fraction of VN for steel VN is 1195×10^{-6} , which includes that nucleated in austenite. The data predicted for the total volume fraction after equalisation at 1200°C for a steel containing 0.001% C is 708×10^{-6} , which is only ~60% of that theoretically possible. Therefore this approach also has shortcomings.

Discussion

Dispersion strengthening

The yield strength of TSDC microalloyed steels is primarily comprised of contributions from the ferrite

Table 3 ChemSage predictions of volume fractions, $f \times 10^6$, of fine precipitates*

	VN	VC	Total V particles	VN/total
0.06 wt-%C				
1050°C	249	1029	1278	0.195
1100°C	450	1029	1485	0.303
1200°C	456	1029	1485	0.307
0.01 wt-%C				
1050°C	302	754	1056	0.286
1100°C	485	754	1239	0.391
1200°C	511	754	1264	0.404
0.001 wt-%C				
1050°C	451	49	510	0.884
1100°C	633	49	682	0.928
1200°C	659	49	708	0.931

*The fine precipitates formed in ferrite at 600°C during cooling, based on steel VN composition, but with three levels of carbon, 0.06, 0.01, 0.001 wt-%, and three equalisation temperatures, with AlN active.

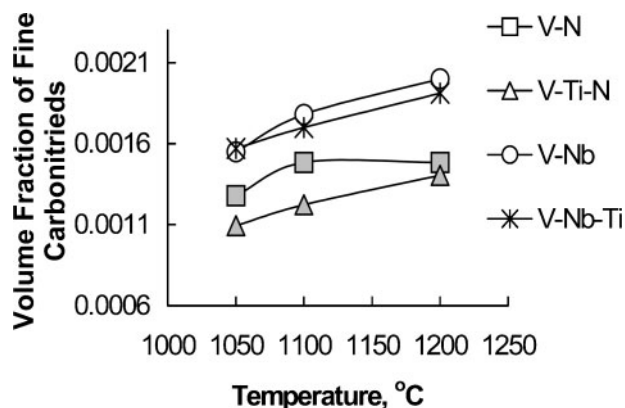
grain size and dispersion strengthening. The small ferrite grain size recorded in this work, Fig. 3 and Table 2, combined with the large dispersion strengthening contribution, Fig. 2 and Table 2, results in yield strength values which can exceed 600 MPa, with satisfactory toughness, also shown in Table 2.

Dispersion strengthening in steel is dependent on the volume fraction, particle size and interparticle spacing of fine particles in ferrite. The size and interparticle spacing of the fine particles are controlled by the nucleation, growth and coarsening rates. The essential parameter governing the variation in nucleation rate is the chemical driving force for precipitation, while that governing growth and coarsening is the diffusion rate. Increasing the vanadium content increases the volume fraction of the fine particles since the high solubility of V(C,N) in austenite allows almost all the vanadium present in the steel to be available for precipitation in ferrite. Furthermore, vanadium has a much higher affinity for N than C. By increasing the nitrogen content in the steel, the predicted nucleation of N rich V(C,N) is enhanced. A consequence of this is a dispersion of a high volume fraction of fine V(C,N) particles, with a small interparticle spacing. Therefore, increasing the V and N content of a steel could lead to a more effective strengthening by precipitation.³¹ With the exception of the VN–ZrN system, where the metal atom size ratio is unfavourable for appreciable intersolubility, all the other binary nitrides give rise to extensive homogeneity ranges.³² However, with the TSDC route even in the multiple microalloyed steels, the fine particles in ferrite are essentially V rich nitrides.^{9,18,20} Hence the volume fraction of fine particles will rely mainly on the amounts of V and N which are available to precipitate in ferrite. Figure 4 shows the size range in a distribution of particles of VN responsible for dispersion strengthening. The average size is ~7 nm. However, it should be noted that the accuracy of the particle measurements, particularly those <5 nm, could be around $\pm 50\%$. The inhomogeneous nature of the distribution of the fine particles shown in Fig. 6 is considered to arise from interdendritic segregation at the as cast stage, which is retained through the entire process.³³ Similar inhomogeneous distributions of particles have been observed, for example, NbC in both stainless steels³⁴ and HSLA steels,³⁵ but the inhomogeneity is invariably ignored in most of the microalloy steels literature or considered to be an artifact arising from the specimen preparation.

Equations (1)–(4) allow values of $\sigma_p + \sigma_d$ to be estimated from a method based on the Hall–Petch relationship. However, assuming the precipitates are incoherent, which the size suggests, then σ_p can be calculated from the Ashby–Orowan equation,¹ which for iron alloys is given by Gladman⁴ as

$$\sigma_p(\text{MPa}) = \frac{10.8f^{1/2}}{d} \ln \frac{d}{6.125 \times 10^{-4}} \quad (5)$$

where *f* is the volume fraction of particles and *d* the average particle diameter in micrometres. Figure 8 shows the calculated volume fraction of carbonitride particles in ferrite which are considered to produce dispersion strengthening. Taking steel V–N as an example, Fig. 8 indicates that following an equalising treatment at 1100°C, *f* in ferrite is $\sim 13 \times 10^{-4}$. This figure is obtained by calculating the total volume



8 Calculated volume fraction of fine precipitates in ferrite for four steels as a function of equalisation temperature

fraction of particles which could form and subtracting that which, under equilibrium conditions, precipitated in austenite before the $\gamma \rightarrow \alpha$ transformation temperature, which is $\sim 760^\circ\text{C}$.

Taking d as 6.5 nm and substituting in equation (5) for f and d gives σ_p as 141 MPa.

$$[\sigma_p(\text{MPa}) = 10.8 \times (0.0013)^{1/2} / (6.5 \times 10^{-3}) \ln(6.5 \times 10^{-3} / 6.125 \times 10^{-4})]$$

Thin foil observations confirm that low dislocation densities ρ were present in the final product of steel V-N. This indicates that ρ was $\leq 10^9$ lines cm^{-2} .

For iron alloys³⁶

$$\sigma_d(\text{MPa}) = 16.2 \times 10^{-4} \rho^{1/2} \quad (6)$$

where ρ is the dislocation density in lines cm^{-2} .

Therefore when ρ is $\sim 10^9$ lines cm^{-2} , $\sigma_d = 51$ MPa, giving $\sigma_p + \sigma_d = 192$ MPa.

This value is at the top end of the range of $\sigma_p + \sigma_d$ in Table 2, and should be compared with the indirect calculation of 163 MPa. The dislocation density would need to reach $\sim 10^{10}$ lines cm^{-2} before a similar contribution to that from σ_p is found. When ρ is 10^{10} lines cm^{-2} , $\sigma_d = 162$ MPa.

The effect of processing parameters on mechanical properties was considered in earlier papers.^{8,9,15} Equalisation temperature is important in relation to the solution temperatures which are respectively for steel V, 1050°C , steel V-N, 1106°C , steel V-Ti, 1443°C , steel V-Nb, 1189°C , steel V-Nb-Ti, 1389°C and steel V-Zr, 1655°C ,³⁷ 1732°C .³⁸ Therefore in these steels the lowest equalisation temperature used in the present work, 1050°C , is predicted to leave some vanadium based particles undissolved in austenite in all but steel V. In the case of steel V-N, the strongest effect on $\sigma_p + \sigma_d$ would appear to be through the end cool temperature (ECT) as can be seen in Table 2. For equalisation temperatures below the solution temperature of the nitrides, i.e. 1050 and 1100°C , it can be seen that $\sigma_p + \sigma_d$ increases with decreasing ECT. With an equalisation temperature of 1050°C , lowering the ECT from 764 to 602°C almost doubles the $\sigma_p + \sigma_d$ to 200 MPa.

Nitride versus carbonitride

The historical perception for vanadium microalloyed steels undergoing a decomposition to ferrite has been summarised by Siwecki *et al.*³⁹ It is often stated that

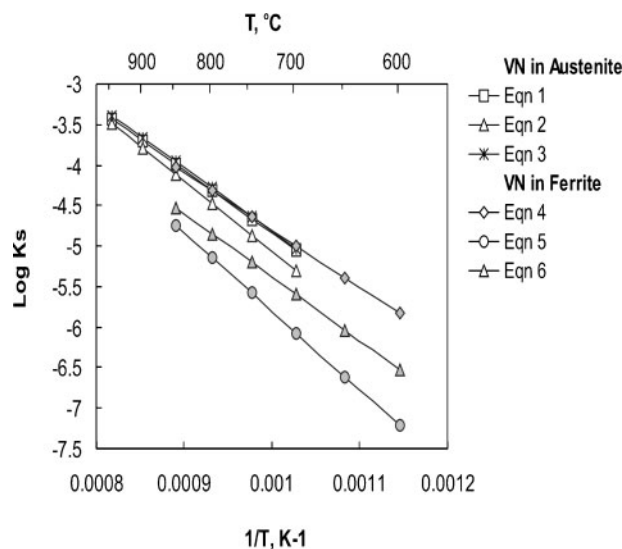
unless the nitrogen level is $< 0.005\%$, initially a high nitrogen carbonitride is formed.⁴⁰⁻⁴⁷ This precipitate was considered to probably nucleate in austenite and was comprised of a nitride rich core with an intermediate carbonitride layer, followed by a carbide outer case. Theoretically, when all the nitrogen is consumed, the remaining vanadium should combine with carbon. Some publications have considered the nitride to nucleate in austenite and the carbide to nucleate in ferrite. In conventional rolled V-Ti or Nb-Ti steels, experimental observations have reported that the complex Ti-V and Nb-Ti particles frequently had a Ti rich nitride core plus hemispherical caps or a carbide coating/shell (V or Nb rich).⁴⁸⁻⁵¹ These characteristics were not present in any of the particles studied in the current work. They are normally found in much larger particles than those being considered here.

Siwecki *et al.*³⁹ in their work, showed by indirect means based on differences in an observed lower contribution to the yield strength, that the core/layers model was not followed in practice. They explained this result by suggesting that either the lower thermodynamic stability of vanadium carbide relative to vanadium nitride is reflected in strongly decelerated precipitation kinetics for the former, or that vanadium carbide coarsens more rapidly, resulting in the observed lower contribution to the yield strength. Further work at the Swedish Institute of Metals, using a ThermoCal software package, modelled the equilibrium solubility of vanadium carbonitride as a function of temperature, for several levels of nitrogen.⁵² The model predicted that for a steel with 0.1%C, 0.1%V and 0.02%N, the vanadium particles present in austenite at 900°C would be essentially VN containing $< 5\%$ C. This compares well with the data for steel V-N given in Fig. 7a, which has similar levels of V and N, but 0.06 wt-%C. In the present work, for steel V-N, it is predicted that the $\gamma \rightarrow \alpha$ transformation temperature is $\sim 760^\circ\text{C}$, and that VN, close to stoichiometry, commences to precipitate once ferrite is formed. In the authors' EELS analysis of steel V-N, fine vanadium nitride precipitates containing little C were found. The complex vanadium nitride/carbonitride/carbide particles hypothesised by some were not present. As an explanation for the authors' observations, this only leaves decelerated precipitation kinetics of vanadium carbide relative to vanadium nitride, under the conditions of the simulated thin slab casting and direct charging.

A recent paper by Maugis and Gouné⁵³ has considered the precipitation of vanadium carbonitride in a steel containing 0.19C, 0.215V and 0.015N (all wt-%). The ratio of the interstitial atoms is $C/N = 15$. This modelling paper again assumed both a vanadium nitride/carbonitride/carbide complex particle and a local equilibrium at the precipitate/matrix interface and considers only precipitation in austenite. The calculations show that for isothermal heat treatment conditions in austenite, 'the precipitates nucleate as almost pure vanadium nitrides. They subsequently grow at the expense of solute nitrogen. When the nitrogen is exhausted, the solute carbon precipitates and progressively transforms the nitrides into carbonitrides.' In addition, they calculated that for an isothermal treatment at 800°C , 'the initial critical radius of nucleation is ~ 0.3 nm, and that after ~ 20 s, the composition of the

solid solution reaches a value where the nucleation rate is practically zero and nucleation stops'. In the present work, owing to the lower carbon content of the steels of ~ 0.06 wt-% compared with 0.19 wt-% used by Maugis and Gouné,⁵³ the ratio of C/N is significantly lower at ~ 4 , which would be expected to enhance the probability of VN precipitation preceding that of carbonitride formation. Also, the present authors considered that VN nucleation commences when the first ferrite is formed, $\sim 760^\circ\text{C}$. The measured cooling rate of 18 K s^{-1} from 760°C to the end cool temperature, then defines the time for precipitation, before the water sprays in effect quench the steel. For steel V-Ti, equalised at 1100°C , which has the lowest end cool temperature given in Table 2, 537°C , the sample took ~ 13 s to reach the end cool temperature. A time of 13 s is well within the 20 s calculated by Maugis and Gouné for a nucleus of mostly VN to precipitate under isothermal conditions at 800°C .⁵³ In addition the diffusion rate of vanadium in ferrite, the rate determining factor for the nucleation of VN, is decreasing as the temperature falls from 760°C to the end cool temperature, which will have a significant effect on the particle growth. Using the data collected by Gladman,⁴ it is estimated that the decrease in the rate of diffusion of vanadium in ferrite between 760 and 537°C is 1.6×10^4 times. Maugis and Gouné⁵³ also comment on the importance of the decrease in solubility of VC in austenite and ferrite, shown in Fig 2 of their paper. However, they do not comment on the solubility of VN in austenite and ferrite, and neither does Gladman,⁴ as the data for VN in ferrite is not included in his book. A good collection of VN solubility equations is given by Rose.⁵⁴ Table 4 shows the results of calculations using the three different equations available for the solution temperatures of VN in both austenite and ferrite^{38,55-58} This data is plotted in Fig. 9. As an example, taking the data for the constants A and B from equations (1) and (6) in Table 4 as the best fit, for the solubility of VN in austenite and ferrite respectively, it is found that the decrease in solubility of VN in γ and in α at 760°C is ~ 3.4 , i.e. the ratio of $2.54 \times 10^{-5}/7.4 \times 10^{-6}$, which is significant, but not substantial.

The thermodynamic modelling approach which provides the best agreement with the authors' modelling, as shown in Fig. 7a, for the situation at the transformation temperature and the present experimental data, is that undertaken by Roberts and Sandberg⁵⁶ following the work of Woodhead.⁵⁹ They⁵⁶ considered the separate cases of interphase and random precipitation in ferrite. Both papers concluded that for microalloyed steels with <0.2 wt-%C and levels of N up to 0.02 wt-%, in the case of randomly precipitated particles in austenite or ferrite, they would have a composition close to stoichiometric VN. A regular solution, and equilibrium condition were



9 Solubility of vanadium nitride in austenite and ferrite

assumed by both sets of authors.^{56,59} Using the equations derived by Roberts and Sandberg⁵⁶ and substituting the chemical composition for steel V-N, for precipitation in ferrite at 600°C , it is predicted that the particle composition would be $\text{V}(\text{C}_{0.01}\text{N}_{0.99})$.

As mentioned above, one of the interesting observations in the present work is the relatively narrow size distribution of VN type particles considered to be associated with a large contribution to the yield strengthening.^{8,9} For example, in the final 7 mm strip of steel V-N, following equalising at 1050°C , as shown in Fig. 4, the average particle diameter, d_{ave} was 6.5 nm and the distribution showed a single peak, skewed towards the smaller particle sizes. The cut-off was $>3d_{\text{ave}}$. This strongly suggests that the particles had not coarsened during processing. Owing to the high cooling rate of the strip, only ~ 13 s elapsed between the FRT and the end cool temperature (Table 1). It is considered that this observation again points to the major fraction of dispersion strengthening particles nucleating during this time. While no detailed work appears to have been undertaken on recrystallisation kinetics of as rolled vanadium microalloyed steels, Zajac *et al.*³¹ have studied precipitation kinetics during isothermal transformation. Kwon and DeArdo⁶⁰ have considered the precipitation and recrystallisation kinetics of niobium steels following high temperature compression testing. Testing at 1000°C resulted in a bimodal particle distribution, which the authors consider to be indicative of particle coarsening, with the smaller particles showing a $d_{\text{ave}} < 12$ nm, while the larger had a d_{ave} of ~ 20 nm, which coincided with coarsening. Similar results for niobium steels were reported more recently by Datta *et al.*,²⁷ who concluded that coarsening occurred in both the deformed and

Table 4 Calculated solubility parameters A and B for VN in austenite and ferrite using equation*

Austenite				Ferrite			
Equation	A	B	Reference	Equation	A	B	Reference
1	-7700	2.86	55	4	-9720	3.90	55
2	-8700	3.63	38	5	-7061	2.26	57
3	-7840	3.02	56	6	-7830	2.45	58

* $\log_{10} K_s = A/T + B$, where K_s is the solubility product $[\text{V}][\text{N}]$ and T the temperature in degrees, K. Equation numbers relate to Fig. 9.

undeformed conditions in specimens held at 950°C. Coarsening coincided with particle diameters of about 20 and 60 nm after holding around 10 and 100 s respectively. All these average particle diameters are significantly larger than the average 6 to 7 nm particle size measured in the present work. Furthermore, bimodal distributions of small particles were not observed in the current work. It is suggested that the present TSDC processing conditions involving high cooling rates, resulted in fine scale segregation in the as cast steel which was retained through to the final product. The high cooling rates following rolling also depress the $\gamma \rightarrow \alpha$ transformation temperature, which is also known to increase the lower yield strength.⁶¹ It is considered that this resulted in the heterogeneous distribution of a high volume fraction of fine incoherent dispersion hardening particles, which in the present work produced a contribution to the yield strength in the range 80–250 MPa. The particles were essentially high nitrogen vanadium nitrides, randomly distributed, which because they did not coarsen, are considered to have nucleated in ferrite.³¹ Particles of VC were not found in any of the steels. The chemical analysis giving only a VN particle, with no transformation layer from a VN core to a rim of VC, is in contradiction to the model often used to support the hypothesis that VN acts as a nucleus for VC precipitation in ferrite, as suggested again in a recent paper.⁵³

The present observations fit much better with the ChemSage predictions, as shown in Fig. 7, for the particle composition associated with equilibrium precipitation of vanadium nitride at the $\gamma \rightarrow \alpha$ transformation temperature of $\sim 760^\circ\text{C}$, for a steel of 0.02 wt-%N and the earlier work of both Roberts and Sandberg⁵⁶ and Woodhead.⁵⁹

Therefore in the authors' work, it is shown that owing to the chosen steel compositions combined with the processing conditions used in the laboratory simulation of direct charged thin slab casting, the particle composition close to VN is observed.

Furthermore, in this study, a lack of evidence of either strain induced precipitation in deformed austenite or interphase precipitation, supports the view that the fine random precipitation occurs in ferrite.³¹

Conclusions

A study simulating thin slab continuous casting followed by direct charging into an equalisation furnace has been undertaken based on six low carbon (0.06%) vanadium microalloyed steels. It is concluded that:

1. Mechanical and impact test data showed that properties were similar or better than those obtained from similar microalloyed conventional thick cast as rolled slabs.

2. The dispersion plus dislocation strengthening was estimated to be in the range 80–250 MPa.

3. A detailed TEM/EELS analysis of the dispersion sized particles, 4–15 nm, showed that in all the steels, they were essentially nitrides with little crystalline carbon detected. In the steels V–Nb, V–Ti and V–Nb–Ti, mixed transition metal nitrides were present.

4. Modelling of equilibrium precipitates in these steels, based on a modified version of ChemSage, predicted that only VN would precipitate in austenite

but that the C/N ratio would increase through the two phase field and in ferrite.

5. The experimental analytical data clearly point to the thin slab direct charging process, which has substantially higher cooling rates than conventional casting, nucleating non-equilibrium particles in ferrite which are close to stoichiometric nitrides. These did not coarsen during the final stages of processing, but retained their highly stable average size of ~ 7 nm, resulting in substantial dispersion strengthening.

Acknowledgements

The authors would like to thank the following: EPSRC, for financial support under grants GR/M22888, GR/M22918; Corus Group PLC, for financial support, VANITEC, also for financial support. The many useful discussions and advice given by Dr W. B. Morrison is acknowledged, as is the help given by Professor D. Gorman.

References

1. E. Orowan: Proc. Symp. on 'Internal stresses in metals and alloys', 451; 1948, London, Inst. Metals.
2. M. F. Ashby: 'Oxide dispersion strengthening', (ed. G. S. Ansell et al.), 143–205; 1958, Warrendale, PA, Met. Soc. AIME.
3. T. Gladman, B. Holmes and I. D. McIvor: 'Effect of second phase particles on the mechanical properties of steel', 68–78; 1971, London, Iron Steel Institute.
4. T. Gladman: 'The physical metallurgy of microalloyed steels', 52; 1997, London, Inst. Materials.
5. E. O. Hall: *Proc. Phys. Soc. London B*, 1951, **64B**, 747–753.
6. N. J. Petch: *J. Iron Steel Inst.*, 1953, **174**, 25–28.
7. J. D. Grozier: Proc. Conf. Microalloying '75, 241–250; 1977, New York, Union Carbide Corp.
8. Y. Li, D. N. Crowther, P. S. Mitchell and T. N. Baker: *ISIJ Int.*, 2002, **42**, 636–644.
9. Y. Li, J. A. Wilson, D. N. Crowther, P. S. Mitchell, A. J. Craven and T. N. Baker: *ISIJ Int.*, 2004, **44**, 1093–1102.
10. R. Kaspar, N. Zentarar and J. C. Herman: *Met. Work.*, 1994, **65**, 279–283.
11. R. Kaspar and O. Pawelski: Proc. Int. METEC Cong., Dusseldorf, Germany, June 1994, VDEH, 390–404.
12. P. J. Lubensky, S. L. Wigman and D. J. Johnson: Proc. Conf. Microalloying '95, 225–233; 1995, Pittsburgh, PA, Iron & Steel Soc.
13. V. Leroy and J. C. Herman: Proc. Conf. Microalloying '95, 213–223; 1995, Pittsburgh, PA, Iron & Steel Soc.
14. M. Korchynsky: *Scand. J. Metall.*, 1999, **28**, 40–45.
15. D. N. Crowther, Y. Li, T. N. Baker, M. J. W. Green and P. S. Mitchell: 'Thermomechanical processing of steels', 527–536; 2000, London, IOM.
16. P. H. Li, A. K. Ibraheem and R. Priestner: *Mater. Sci. Forum*, 1998, **284–286**, 517–524.
17. Y. Li, D. N. Crowther, J. A. Wilson, A. J. Craven and T. N. Baker: *IOP Conf. Ser.*, 2001, **168**, 183–186.
18. J. A. Wilson, A. J. Craven, Y. Li and T. N. Baker: *IOP Conf. Ser.*, 2001, **168**, 187–190.
19. T. N. Baker, Y. Li, J. A. Wilson, A. J. Craven and D. N. Crowther: *Mater. Sci. Technol.*, 2004, **20**, 720–730.
20. Y. Li and T. N. Baker: *Mater. Sci. Forum*, 2005, **500–501**, 237–244.
21. A. Cracknell and N. J. Petch: *Acta. Metall.*, 1955, **3**, 186–189.
22. F. B. Pickering and T. Gladman: 'Metallurgical developments in carbon steels', ISI Spec. Rep. no. 81, Iron Steel Inst., London, UK, 1963.
23. W. C. Leslie: *Metall. Trans.*, 1972, **3**, 5–36.
24. W. B. Morrison and J. A. Chapman: Proc. Rosenhain Centenary Conf., 286–303; 1976, London, The Royal Society.
25. A. J. Rose: 'Methods of measurement of precipitation in steels', Rep. SL/PM/R/S2971/17/98/A, British Steel Plc, Swinden Technology Centre, 1998.
26. B. Dutta, E. J. Palmiere and C. M. Sellars: *Acta. Metall. Mater.*, 1992, **40**, 653–662.

27. B. Datta, E. J. Palmiere and C. M. Sellars: *Acta Mater.*, 2001, **49**, 785–794.
28. W. J. Liu and J. J. Jonas: *Met. Trans. A*, 1995, **26A**, 1641–1657.
29. M. G. Akben, I. Weiss and J. J. Jonas: *Acta Mater.*, 1981, **29**, 111–121.
30. D. H. Bratland, Ø Grong, H. Shercliff, O. R. Myhr and S. Tjøtta: *Acta Mater.*, 1997, **45**, 1–22.
31. S. Zajac, T. Siwecki and M. Korchynsky: 'Low-carbon steels for the 90's', (ed. R. Asfahani and G. Tither), 139–149; 1993, Warrendale, PA, TMS.
32. H. J. Goldschmidt: 'Interstitial alloys', 238; 1957, London, Butterworths.
33. K. Douse and T. N. Baker: 'Thermomechanical processing of steels', 573–580; 2000, London, IOM.
34. C. Y. Barlow, B. Ralph, B. Silverman and A. R. Jones: *J. Mater. Sci.*, 1979, **4**, 423–430.
35. R. M. Poths: 'Factors influencing the precipitation of Nb–CN during the thermomechanical processing of microalloyed steel', PhD thesis, University of Sheffield, UK, 2003.
36. T. N. Baker: 'Yield, flow and fracture', (ed. T. N. Baker), 235–273; 1983, London, New York, Applied Science Publishers.
37. D. B. Evans: *Trans. Met. Soc. AIME*, 1965, **233**, 1620–1624.
38. K. Narita: *Trans. ISIJ*, 1975, **15**, 145–152.
39. T. Siwecki, A. Sandberg, W. Roberts and R. Lagneborg: 'Thermomechanical processing of austenite', (ed. A. J. de Ardo *et al.*), 163–194; 1982, Warrendale, PA, Met. Soc. AIME.
40. H. A. Vogels, P. Konig and K.-H. Piehl: *Archiv. Eisenh.*, 1964, **35**, 339–351.
41. T. N. Baker: *J. Iron Steel Inst.*, 1973, **211**, 502–510.
42. T. N. Baker: *Met. Technol.*, 1974, **1**, 126–131.
43. D. C. Houghton, G. C. Weatherly and J. D. Embury: 'Thermomechanical processing of austenite', (ed. A. J. de Ardo *et al.*), 267–292; 1982, Warrendale, PA, Met. Soc. TMS-AIME.
44. W. Roberts: 'HSLA steels, technology and applications', (ed. M. Korchynsky), 33–65; 1984, Metals Park, OH, ASM.
45. J. Strid and K. E. Easterling: *Acta Metall.*, 1985, **33**, 2057–2074.
46. F. Sun and W. Cui: 'HSLA steels, processing, properties and technology', (ed. G. Tither and S. Zhang), 43–50; 1992, Warrendale, PA, TMS-AIME.
47. T. Gladman: 'HSLA steels, processing, properties and technology', (ed. G. Tither and S. Zhang), 3–14; 1992, Warrendale, PA, TMS-AIME.
48. T. Siwecki, A. Sandberg and W. Roberts: 'HSLA steels, technology and applications', (ed. M. Korchynsky), 619–634; 1984, Metals Park, OH, ASM.
49. K. He and T. N. Baker: *Mater. Sci. Eng. A*, 1993, **A169**, 53–65.
50. R. L. Bodnar, Y. Shen and V. Furdanowicz: *Iron Steelmaker*, 1999, **26**, 45.
51. R. M. Poths, R. L. Higginson and E. J. Palmiere: *Scr. Mater.*, 2001, **44**, 147–151.
52. S. Zajac: Proc. 43rd MWSP Conf., Vol. 29, 497–508; 2001, Warrendale, PA, ISS.
53. P. Maugis and M. Gouné: *Acta Mater.*, 2005, **53**, 3359–3567.
54. A. Rose: 'Modelling the precipitation in microalloyed steels', British Steel Report SL/PM/R/S2971/4/97/A, UK, 1979.
55. E. T. Turkdogan: *Trans ISS, Iron and Steelmaker*, 1989, May, 61–75.
56. W. Roberts and A. Sandberg: 'The compositions of V(C,N) as precipitated in HSLA steels microalloyed with vanadium', Swedish Institute for Metals Report no. IM-1489, Stockholm, Sweden, 1980.
57. V. Raghavan: *Bull. Alloy Phase Diag.*, 1984, **5**, 194–198.
58. M. G. Froberg and H. Graf: *Stahl und Eisen*, 1960, **80**, 359–364.
59. J. H. Woodhead: Proc. Seminar on 'Vanadium in high strength steel', 3–10; 1979, London, VANITEC.
60. O. Kwon and A. J. de Ardo: *Acta Metall. Mater.*, 1991, **39**, 529–538.
61. J. H. Bucher and J. D. Grozier: *Met. Eng. Quart. Am. Soc. Met.*, 1965, **5**, 1–6.